Molecular Dynamics Simulation of the Energetics and Structure of Layered Double Hydroxide Intercalated with Carboxylic Acids

ARTICLE · JANUARY 2007

READS
30

3 AUTHORS, INCLUDING:

Padmanabhan Padma Kumar
Indian Institute of Technology Guwahati
33 PUBLICATIONS **632** CITATIONS
SEE PROFILE

Andrey G. Kalinichev
École des Mines de Nantes
117 PUBLICATIONS **2,922** CITATIONS
SEE PROFILE

Molecular Dynamics Simulation of the Energetics and Structure of Layered Double Hydroxides Intercalated with Carboxylic Acids

P. Padma Kumar,* Andrey G. Kalinichev, and R. James Kirkpatrick

Department of Geology, University of Illinois at Urbana-Champaign, 245 Natural History Building, 1301 West Green Street, Urbana, Illinois 61801

Received: April 25, 2007; In Final Form: June 27, 2007

Molecular dynamics (MD) simulation of the Mg/Al (3:1) layered double hydroxide (LDH), hydrotalcite (HT), containing the monocarboxylic acids formate, acetate, and propanoate as the charge balancing interlayer anions provides new molecular-scale insight into the interlayer structure, hydrogen bonding, and energetics of hydration and consequent swelling of LDH compounds containing organic molecules and biomolecules with carboxylate functional groups. As for citrate−HT (Kumar, P. P.; Kalinichev, A. G.; Kirkpatrick, R. J. *J. Phys. Chem. B* **2006**, *110*, 3841), the hydration energy of these systems as a function of water content has no distinct minima, indicating the absence of energetically well-defined structural states with specific water contents. The hydration energies, however, approach the energy of bulk liquid water at lower water contents than for citrate−HT, suggesting that synthesis strategies involving delamination of the hydroxide layers in water are likely to be more successful using starting compounds containing larger molecules with multiple carboxylate groups. This result is consistent with recent experimental observations of the delamination of lactate−HT (Hibino, T.; Kobayashi, W. *J. Mater. Chem.* **2005**, *15*, 653. Jaubertie, C.; Holgado, M. J.; San Roman, M. S.; Rives, V. *Chem. Mater.* **2006**, *18*, 3114). The structural behavior of carboxylate anions in LDH interlayers is directly related to the energetic relationships, with electrostatic interactions and the H-bonding between the -COO^- sites of the anions, the M−OH sites of the metal hydroxide sheets, and the interlayer H_2O molecules playing dominant roles. The hydrogen bonds donated to the anions from water molecules are energetically preferable to those from M−OH sites, resulting in decreasing occurrence of the anions in inner-sphere coordination environments to the hydroxide sheets with increasing water content.

1. Introduction

Layered double hydroxides (LDHs) are claylike phases with positive structural charge due to allovalent substitution in the metal hydroxide layers. They are readily synthesized with a variety of charge-balancing anions incorporated into their interlayers along with associated water molecules.[1,2] By virtue of their expandable interlayers along the crystallographic *c*-dimension (perpendicular to the layers), LDHs serve as excellent hosts for a broad range of organic and inorganic charge-balancing anions and a variety of neutral chemical species. This makes them useful in a wide range of applications in such diverse fields as catalysis,[3−6] photochemistry,[3,6] electrochemistry,[3,6,7] medicine,[4,7−9] molecular separation, and environmental chemistry.[3,4,8,10]

Incorporation of organic molecular and biomolecular species into the interlayers of layered double hydroxide compounds (LDHs) has gained increasing attention in recent years due to their potential applications in controlled drug delivery systems[11−15] and environmental remediation.[8,10] Intercalation of large organic molecules into LDH interlayers can be difficult, but recent experimental studies have shown that enhanced swelling leading to exfoliation (delamination) of the LDH layers can be achieved in contact with a solution if the LDH is loaded with suitable organic intercalates.[16−19] Such exfoliation offers a gentle way of opening the interlayer space to allow insertion of large organic or biomolecules. Recent experimental and computational molecular dynamics (MD) modeling studies of citrate[20,21] (a carboxylic acid) and glutamate[22,23] (an amino acid with a carboxylic tail) are consistent with these results and suggest that the interaction energies of such species with the LDH structure are weaker than those of small inorganic anions such as Cl^-, CO_3^{2-}, and SO_4^{2-},[24] allowing for larger expansions and potentially delamination in water.

This paper presents the results of a computational MD study of the LDH compound hydrotalcite containing the small monocarboxylic anions formate $(CHO_2)^-$, acetate $(C_2H_3O_2)^-$, and propanoate $(C_3H_5O_2)^-$ that provides significantly increased molecular-scale insight into the structural and energetic origins of the interactions of organic molecules containing carboxylate functional groups with LDH compounds. Combined with our earlier MD simulations of citrate−intercalated HT,[21] these results support the concept that carboxylate sites interact relatively weakly with LDH layers and that large expansions leading to delamination in water can be energetically favorable.

2. Methods

The crystal structure of hydrotalcite (HT) is based on that of brucite, $Mg(OH)_2$, but with partial Al^{3+} for Mg^{2+} substitution in the octahedral hydroxide sites. Our computational models use the typical structural formula $Mg_3Al(OH)_8A^-\cdot nH_2O$, where A^- is the anion. The MD simulations were performed for HT supercells consisting of $6 \times 6 \times 1$ rhombohedral ($R\bar{3}m$) unit cells.[25] Each supercell contained three metal−hydroxide layers, 27 carboxylic acid anions (9 per interlayer), and a variable

* Corresponding author. E-mail: padma@uiuc.edu.

10.1021/jp0732054 CCC: $37.00
Published on Web 08/17/2007

number of water molecules, $27n$, where $0 \leq n \leq 18$. The smallest system studied, the dry ($n = 0$) formate−LDH, has a supercell dimension of $18.9 \times 18.9 \times 21.5$ Å. Because of the relatively small size of the supercells, we assumed a completely ordered Mg, Al distribution in the hydroxide layers. Long-range cation ordering in LDHs has been difficult to observe by powder X-ray diffraction, except for the Li/Al and Mg/Ga phases.[25] X-ray absorption spectroscopy, however, indicates the absence of Fe−Fe neighbors in Mg/Fe HT, suggesting domains of cation ordering with dimensions at least a few nanometers.[26] More recently, Génin et al.[27] used Mössbauer spectroscopy to directly demonstrate the existence of long-range cation ordering in a similar $Fe^{II}-Fe^{III}$ LDH phase. Even though such ordering cannot be detected by XRD, they concluded that it is likely to exist in other isomorphous LDHs, such as hydrotalcite.[27]

The carboxylic groups of the formate, acetate, and propanoate molecules intercalated into hydrotalcite are considered to be deprotonated, since all of their pK_a values are less than 5.[28] Thus, they are modeled as the singly charged anion. The MD simulations started from energy- and stress-minimized structures. For all hydration states, n, modeled, *NPT*-ensemble MD simulations of 50 ps duration were carried out at 300 K and 1 bar pressure. The initial 30 ps period of these simulations was used for equilibration, and the average unit cell parameters and hydration energy were calculated over the remaining 20 ps. In addition, detailed structural analysis was undertaken at 300 K for select hydration levels, $n = 0$, 2, 4, and 10, using longer *NVE*-ensemble MD simulations of 200 ps duration, including an initial 50 ps time for equilibration. The starting configurations for these runs were the final atomic configurations and *average* interlayer spacings obtained from the initial *NPT*-MD simulations for the same water content. All MD simulations were performed with a time step of 0.5 fs. Periodic boundary conditions and Ewald summation were employed to account for the long-range electrostatic interatomic interactions. All simulations reported here used the interatomic potentials from the CLAYFF force field of Cygan et al.[29] to describe the LDH layers, the SPC water model of Berendsen et al.,[30] and the CVFF force field[31] to describe the carboxylic species. CVFF is fully compatible with CLAYFF and is broadly applicable to organic species.[32,33]

The energetics of hydration was analyzed via the computed hydration energy defined as

$$\Delta U_{\mathrm{H}}(N_{\mathrm{w}}) = \frac{\langle U(N_{\mathrm{w}})\rangle - \langle U(0)\rangle}{N_{\mathrm{w}}} \qquad (1)$$

where N_w is the total number of water molecules, $U(N_w)$ is the total potential energy of the system, and $U(0)$ is the total potential energy of the system with no water molecules. Previous results have shown that this parameter is a simple and effective measure of the affinity of water for the interlayer;[34,35] Heinz et al.[36] have recently proposed that reproduction of crystal surface and cleavage energies is a useful quantitative criterion to improve and validate the performance of semiempirical force fields used for molecular simulations of organo-inorganic layered nanocomposites. Although CLAYFF was designed to be a relatively simple and broadly applicable force field for oxide and hydroxide systems and was not optimized to reproduce these properties,[29] compared to several other commonly used force fields it actually performs surprisingly well in this regard.[36] Moreover, since the hydration energy in eq 1 represents the energy difference between two structures that differ only by their water content, we expect most of the possible errors due to the inaccuracies of the crystal energy to cancel out in the final analysis. This should be especially true for our simulated systems, since the dominant contributions to the hydration energy arises from the formation of hydrogen bonds between the interlayer water molecules, the hydroxide layers, the interlayer anions, and among the H_2O molecules themselves.

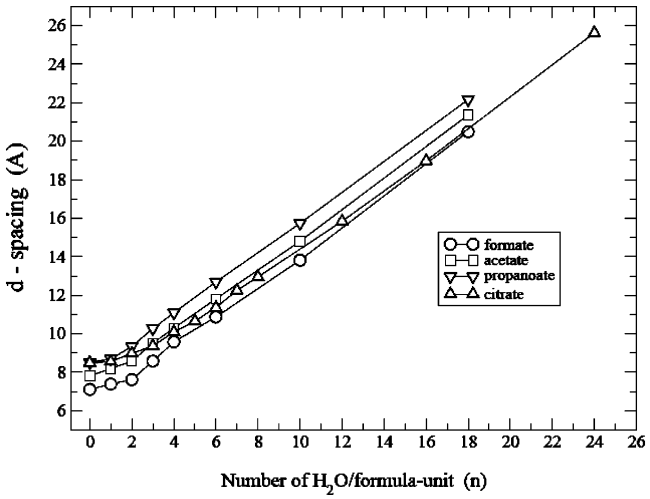

Figure 1. Variation of interlayer spacing (crystallographic *c*-axis length) as a function of the number of water molecules per formula unit, n, from *NPT*-MD simulations at 300 K and 1 bar pressure of formate−, acetate−, propanoate−, and citrate−HT.

For the purpose of the analysis of H-bonds between the different interlayer species with the metal−hydroxide layers as well as among themselves, we use a common H-bond definition[37] in which a hydrogen bond is considered to exist between two species if the donor−acceptor distance is less than 3.5 Å and simultaneously the hydrogen−donor−acceptor angle is less than 30°. Contour maps of atomic probability density parallel to the metal−hydroxide layers and atomic density profiles perpendicular to them, calculated over the long *NVE*-MD trajectories, are used to visualize the interlayer structure.

3. Results and Discussion

3.1. Crystal Structure and Swelling Energetics. The combination of the CLAYFF[29] and CVFF[31] force fields to describe the structure of the organically intercalated LDHs preserves the cell parameters and the symmetry of the crystals quite well. The average *a*- and *b*-unit cell dimensions computed from the *NPT*-ensemble MD simulations are all within 0.2% of each other and are also within 1.5% of the literature values[25] of $a = b = 3.10$ Å at all hydration levels. The average unit cell angles α and β are all within 5° of the ideal value of 90°. The in-plane angle γ is much more robust and varies less than 0.1° from the ideal value of 120°, as expected of a lamellar structure.

The computed basal spacings (*d*-spacings) of formate−, acetate−, and propanoate−HT all increase with increasing water content, n, as expected (Figure 1). As observed for LDHs with both organic and inorganic interlayer anions, the rate of basal spacing increase is less at small water contents as the water molecules fill in space between the anions. For these three systems, the basal spacings increase with increasing anion size, and the trends with increasing n are essentially parallel. In contrast, the rate of increase for citrate−HT is smaller,[21] reflecting the ability of H_2O molecules to form more compact structures around the three -COO^- groups of the larger citrate molecule than around the hydrophobic ends of the monocarboxylate species.

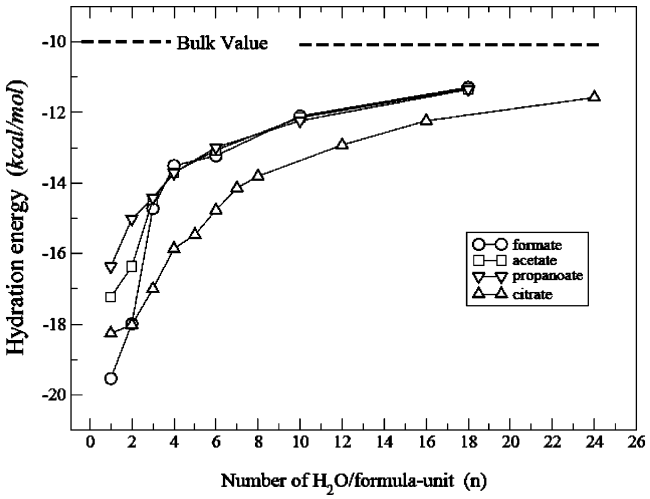

Figure 2. Variation of the system hydration energy (eq 1) as a function of the number of water molecules per formula unit, *n*, from *NPT*-MD simulations at 300 K and 1 bar pressure of formate−, acetate−, propanoate−, and citrate−HT.

The computed hydration energies (eq 1) are most negative at low water contents, with the values increasing with decreasing size of the hydrophobic tails of the monocarboxylate species (Figure 2). The latter trend is expected, because the hydrophobic tails interact unfavorably with the water molecules while also inhibiting water molecules from forming hydrogen bonds with the hydroxide layers. In this respect, citrate falls between formate and acetate, since it has less than one hydrophobic -CH_2- group per carboxylate group. In addition, there are only one-third as many citrates as monocarboxylate species in each LDH interlayer due to charge balance requirements.

For formate−, acetate−, and propanoate−HT, the absolute values of the hydration energies decrease rapidly with increasing water content and within computational error converge to the same values at $n = 3$. With further increase in water content, the $\Delta U_H(N_w)$ values increase at a progressively smaller rate and are the same for all three systems. The hydration energy approaches but does not reach the value characteristic to bulk liquid water (∼−10 kcal/mol for SPC water) over the range of hydration states examined. The trends are qualitatively similar to that for citrate HT (Figure 2), but at $n \geq 3$ the value is less for the citrate phase, suggesting its stronger affinity for water. The trends for the monocarboxylic systems all approach the bulk water value at lower water contents than citrate−HT.

As for citrate−HT,[21] the trends in hydration energy for formate−HT, acetate−HT, and propanoate−HT contain no distinct energy minima over the hydration range explored, indicating the absence of specifically preferred hydration states and a tendency to adsorb water continuously in water-rich environments such as high relative humidity (RH) conditions or in aqueous suspensions. The practical outcome of this relationship is expansion to larger basal spacings or delamination of the layers, as recently observed experimentally for lactate−HT[16,17] and citrate−HT[20] in water. This behavior is in sharp contrast to the computed hydration energetics of chloride−HT found in previous MD studies,[35] and the experimentally known restricted ranges of hydration of HT containing small, inorganic anions.[24]

3.2. Interlayer Molecular Structure and Hydrogen Bonding. Detailed analysis of the computed interlayer structures provides improved molecular-scale understanding of the origins of the energetic trends described above, showing that the most important stabilizing factor is the progressive development of a percolating H-bond network among the metal−hydroxide layers, interlayer anions, and H_2O molecules. A similar detailed picture cannot be obtained from experimental diffraction or spectroscopic data, because of the disordered interlayer structure and the difficulty in locating H-atoms.

In the collapsed interlayers for the dry systems ($n = 0$), the anions interact strongly with the metal hydroxide layer and execute largely local dynamics. The anions bridge the metal hydroxide layers on either side of the interlayer, and the O atoms of the -COO^- groups are H-bonded to the H of the M−OH sites. As for citrate−HT,[21] all of the monocarboxylate ions orient parallel to the layers (Figure 3a−c) in the dry system. Formate−HT has the smallest basal spacing, and acetate and propanoate have larger ones due to their hydrophobic groups. Despite comparable lateral dimensions, propanoate causes a larger basal spacing than acetate because its additional hydrophobic -CH_2- group causes a larger repulsion of the metal−hydroxide layers. The orientation of the -COO^- groups is different for the three different anions. For formate, the -COO^- groups lie parallel to the layering, with both O-atoms coordinated to both hydroxide layers (Figure 3a). For propanoate they lie perpendicular to the layers, with the two O-atoms coordinated to different hydroxide layers (Figure 3c). For acetate, the -COO^- groups are orientationally more disordered and exhibit dynamical switching between these two types of coordinations (Figure 3b).

The atomic density contours (Figure 4) provide valuable insight into the distribution of atomic density in the LDH interlayers and the nature of the interaction between the interlayer species with the metal−hydroxide layers. For dry formate−HT, the O-atoms of -COO^- lie principally on the edges of the M−OH triangles, allowing each O to ideally accept 2 H-bonds from two of the opposing M−OH layers. The dry propanoate−HT is strikingly ordered and the O-atoms of the -COO^- lie directly above the center of the M−OH triangles, allowing each O-atom to accept ideally 3 H-bonds. The acetate phase is more disordered, and the O-atoms of its -COO^- groups that lie parallel to the layers tend to occupy M−OH sites along the H−H vectors, whereas those of -COO^- groups oriented at high angles to the layers tend to occupy the centers of the M−OH triangles. The ordered structure of propanoate−HT (Figure 4c) may be due to the need for efficient packing of the larger propanoate anions to accommodate them with a layer-parallel orientation. This size effect predicts that larger monocarboxylate anions would occur at larger angles to the layers.

The structural relationships for the dry ($n = 0$) phases are reflected directly in the H-bond statistics, which show an average of 7 H-bonds per carboxylate group for formate−HT and about 5.6 for the acetate and propanoate phases (Figure 5). The smaller than ideal values (8 and 6, respectively) reflect structural disorder. These relationships are also clearly reflected in the atomic density profiles perpendicular to the layering (Figure 6). For formate−HT, the O- and C-atoms of the -COO^- groups are all at the same level, reflecting their parallel arrangement. For propanoate−HT, as for citrate−HT, the O-atoms lie next to the hydroxide layers, and the C-atoms are in the center of the interlayer, reflecting the perpendicular -COO^- arrangement. For acetate−HT both situations occur.

With increasing water content, the carboxylate anions progressively change their orientation from parallel to the layers to nearly perpendicular (Figure 3d−i). They also progressively lose nearest neighbor coordination contact with the hydroxide layers and have increasing coordination to H_2O molecules, as shown by their diminished preference for specific M−OH sites (Figure 3d−i). Those water molecules near the metal−hydroxide

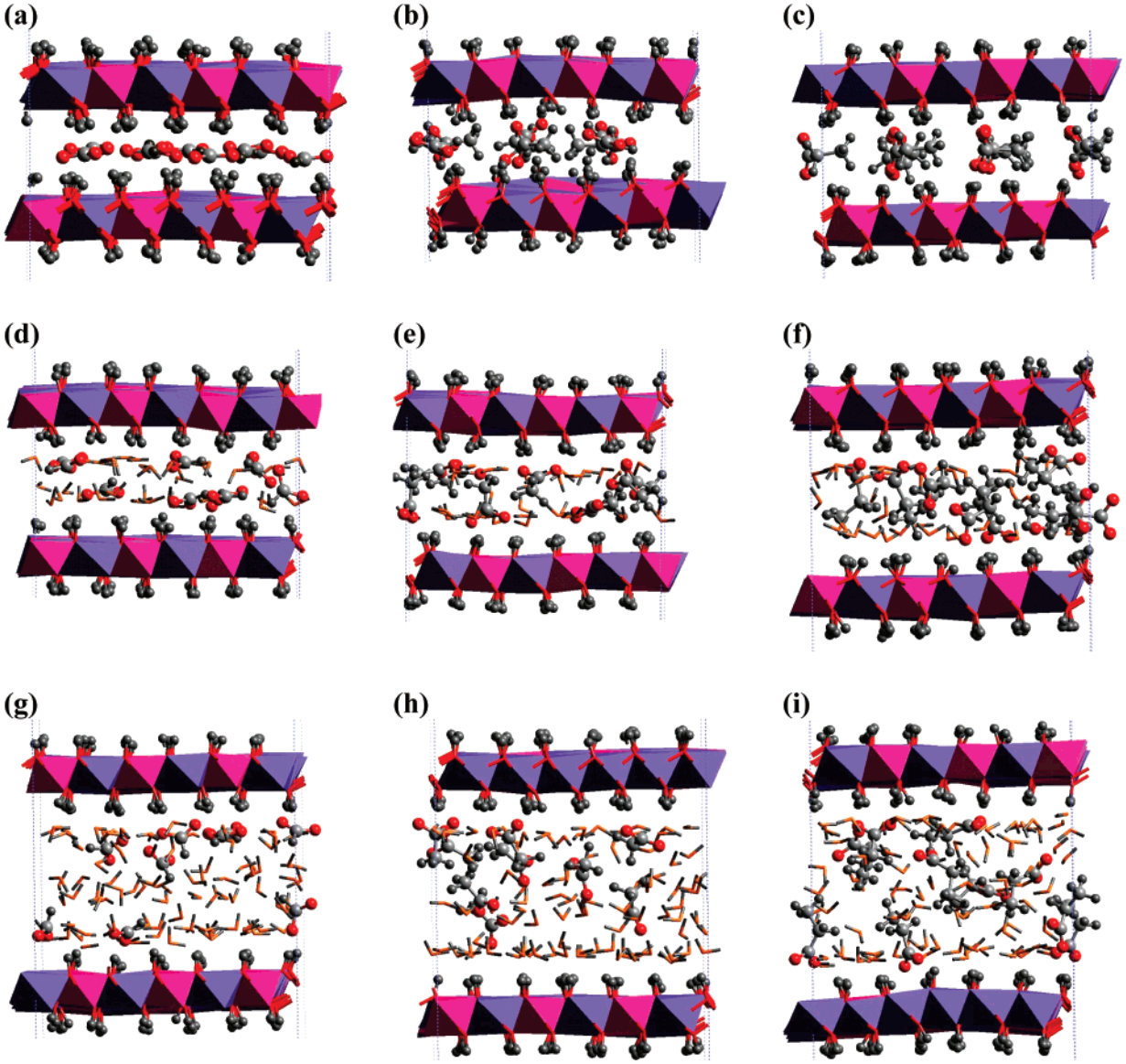

Figure 3. Representative snapshots from MD simulations of hydrotalcite intercalated with formate (left column), acetate (middle column), and propanoate (right column) showing position and orientation of the interlayer species with changing water content. Top row, $n = 0$; middle row, $n = 4$; bottom row, $n = 10$. See text for discussion of the molecular orientations and the decreasing inner sphere coordination of the anions with increasing water content.

layers exhibit strong preference for surface sites directly above M−OH (Figure 4d−i). Water also allows for faster reorientational dynamics of the interlayer species, as reflected in the increasing disorder in the atomic density contours (Figure 4d−i).

At $n = 4$, the atomic density contours plots show a significant number of unoccupied surface sites, suggesting that the orientation of the carboxylate ions at an intermediate angle hinders water molecules from accessing the surface. Parts d−f of Figure 4 show a qualitative picture of this *steric effect* that increases from formate to propanoate. At higher water contents, essentially all surface sites are occupied by water molecules, except those occupied by the -COO^- groups. The steric effect is essentially eliminated due to the vertical orientation of the anions, and the surface is essentially saturated (Figure 4g−i). The result is a quite well ordered hexagonal arrangement of the water molecules, as also observed in MD simulations of the surfaces of many single and double hydroxides.[38,39] The comparatively isolated nature of the atomic density contours of the water oxygens suggests negligible surface diffusion of water. In contrast, the larger overlap of the atomic density contours of the carboxylate−oxygens and water−oxygens at $n = 10$ (Figure 4g−i) suggests faster dynamical exchange of these species among the surface sites at larger water contents.

The changes in interlayer structure of the different HT phases with progressive hydration are closely related to changes in the hydrogen-bonding patterns of the interlayer species. In these systems, the M−OH sites act as pure H-bond donors, the carboxylate anions as pure H-bond acceptors, and the water molecules as both H-bond donors and acceptors. The average number of the H-bonds/-COO^- group accepted by the carboxylate anions from the metal−hydroxide layers, from water, and the sum of the two are shown as functions of the water content in Figure 5. All the anions are undersaturated in H-bonds at $n = 0$, but the total number of H-bonds reaches a saturation value that is similar to bulk aqueous solution by $n = 4$. In the dry state, formate makes an average of 7 H-bonds per carboxylate group, whereas acetate and propanoate form about 5.5 (Figure 5a,b). The saturation value is slightly different for the different carboxylate species, with the formate making a slightly larger number due to its smaller size. Similarly, the total number of H-bonds donated by the M−OH groups reaches a saturation

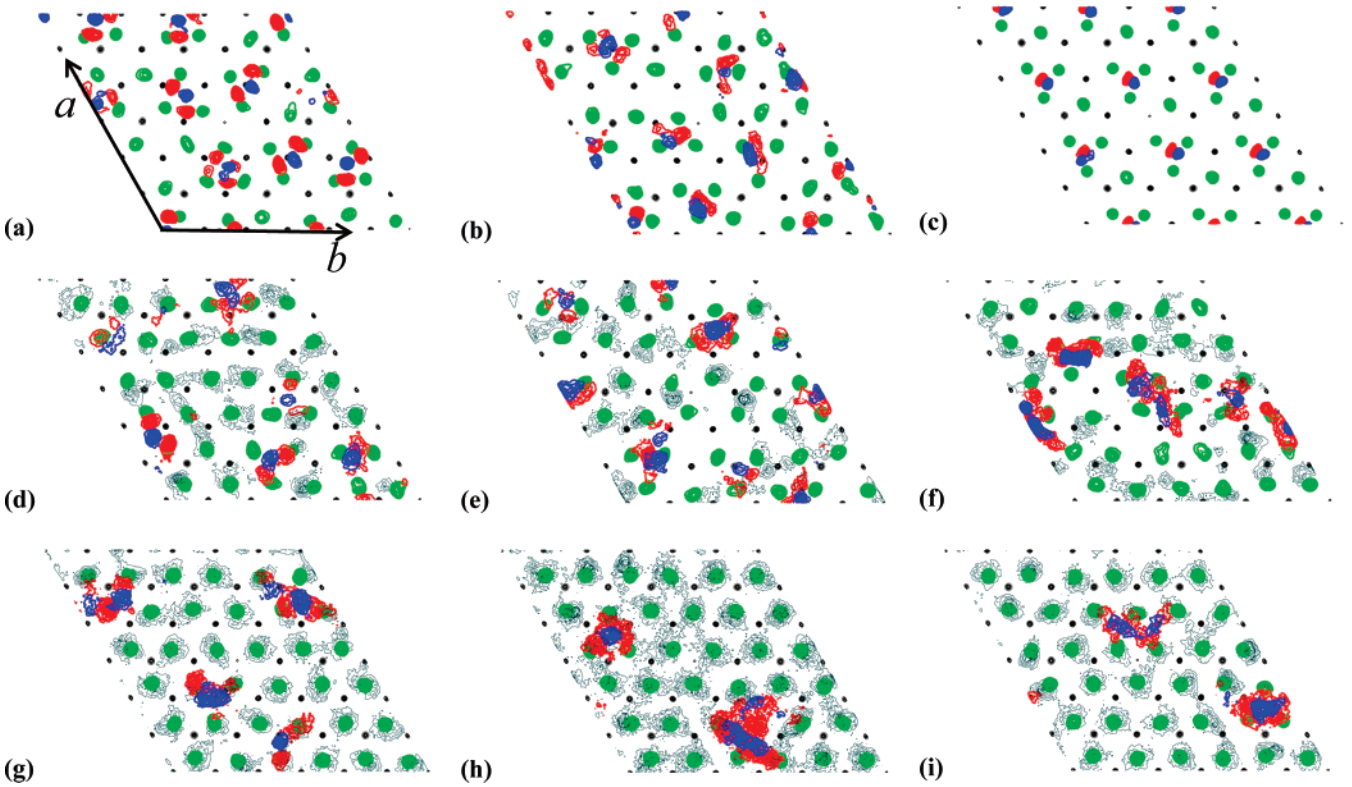

Figure 4. Time-averaged atomic probability density maps of the interlayer species H-bonded to the hydroxyl groups on one side of an arbitrarily chosen layer for formate- (left column), acetate- (middle column), and propanoate-intercalated (right column) hydrotalcite at different water contents. The directions of the unit cell vectors *a*, *b* shown in a is common to all the plots. Top row, $n = 0$; middle row, $n = 4$; bottom row, $n = 10$. Green contours, hydrogens of M−OH groups of the HT structure; red contours, oxygens of carboxyl groups; blue contours, carbons of carboxyl groups; thin light blue contours, oxygens of H_2O molecules.

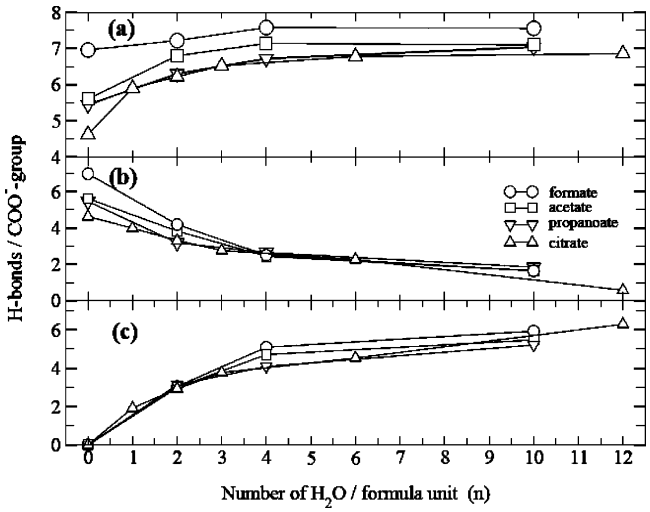

Figure 5. Hydrogen bond statistics for the different anionic species as a function of the number of water molecules per HT formula unit: (a) average number of H-bonds accepted by anions from M−OH and water; (b) average number of H-bonds donated by M−OH to the anions; (c) average number of H-bonds donated by water molecules to the anions.

value of 0.9/OH by $n = 6$. Overall, this change results in a progressive replacement of -COO^- by H_2O as nearest neighbors to the hydroxide surface and a parallel increase in the number of H-bonds donated to H_2O by the M−OH sites and a decrease in the number of H-bonds donated by M−OH to the carboxylate groups of the anions (Figure 5). Citrate exhibits a stronger preference for accepting H-bonds from water at large hydration values ($n > 6$), as reflected in the H-bonding statistics. The absence of H-bond donation by H_2O to the M−OH sites is consistent with previous MD studies of LDH compounds and is due to the attraction of the negative ends of the H_2O molecules to the positive structural charge of the hydroxide layers.[35,38,39]

3.3. Structural Origin of Changes in Hydration Energy. The decrease in computed hydration energy with increasing water content for the formate−, acetate−, propanoate−, and citrate−HTs shown in Figure 2 is the direct result of the changes in the structural rearrangements, *c*-axis expansion, and the H-bonding between the interlayer species. As discussed by Boek et al.,[40] Smith,[34] and Wang et al.,[35] the hydration energy as defined in eq 1 is a good measure of the energetic effects of adding water molecules to an interlayer, and the difference between it and the energy of a molecule in bulk water is a measure of the thermodynamic driving force to transfer a molecule from bulk aqueous solution to the interlayer. $\Delta U_H(N_w)$ reflects not only the changes in the energy of the interlayer water as it interacts with the hydroxide layers, the anions, and other water molecules but also the changes in interaction energy between the hydroxide layers, between the interlayer anions, and between the anions and the hydroxide layers.[35] The details of the individual components of these changes are difficult to quantitatively evaluate, but expansion of the interlayer necessarily increases the system energy, and incorporation of water and associated interlayer reorganization and H-bond formation reduces it.

For the monocarboxylate−HTs, the large negative values of the hydration energy at low water contents reflect a combination of relatively small interlayer expansion as the water molecules occupy sites between the anions and the formation of new H-bonds between these molecules and the unsaturated M−OH and -COO^- sites. As the interlayers expand, the anions lose nearly half of the H-bonds they accept from M−OHs, which

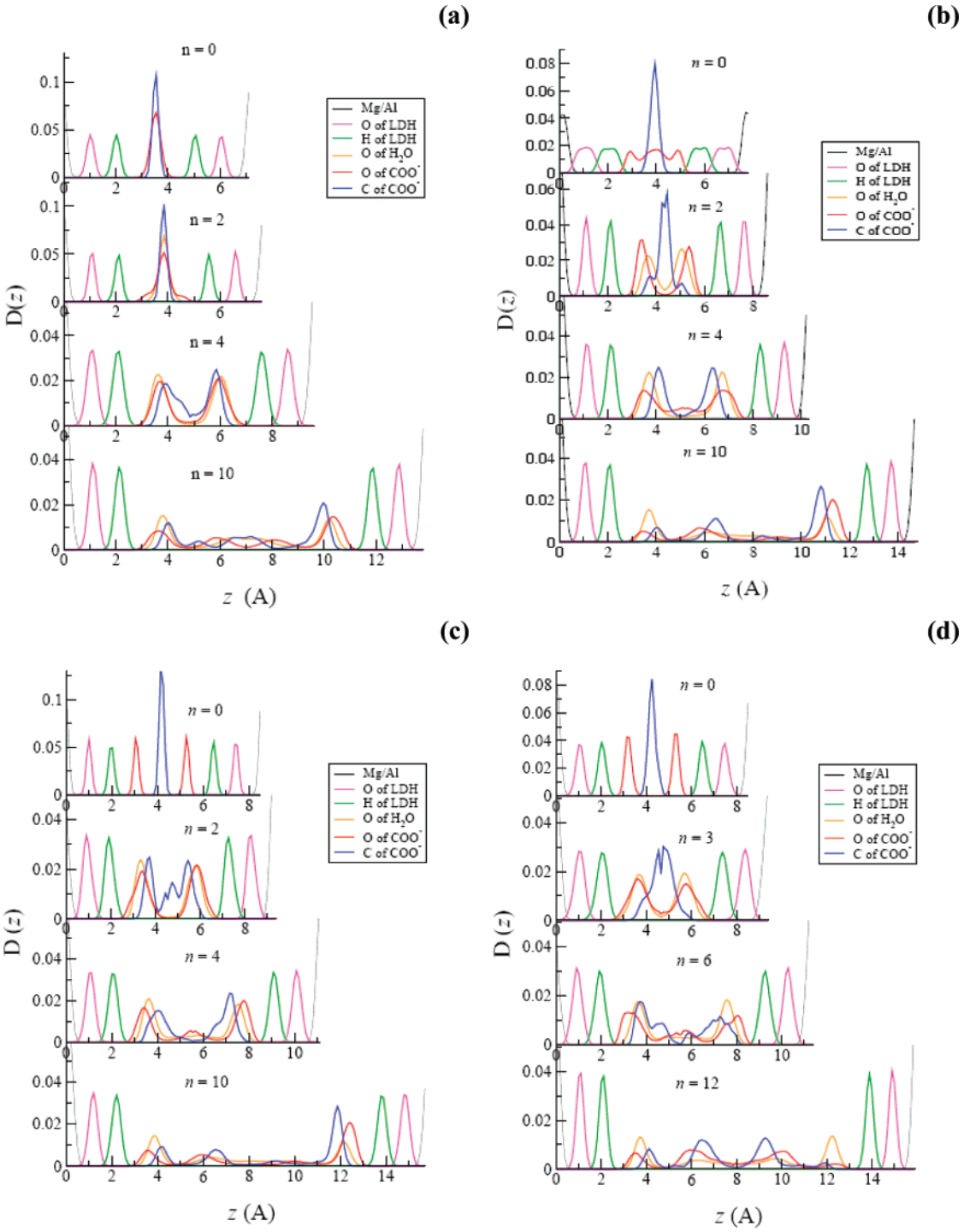

Figure 6. MD-simulated atomic density profiles perpendicular to the hydroxide layers for (a) formate−HT, (b) acetate−HT, (c) propanoate−HT, and (d) citrate−HT as functions of water content. See text for discussion.

are compensated by the added water molecules. Simultaneously, double layers of anions are formed in the interlayer. The water content at which these double layers form decreases with increasing size of the hydrophobic part of the anion. For instance, for propanoate double layers form at $n = 2$, whereas for formate this occurs at $n = 4$. In this regime, the progressive increase in H-bond formation between water molecules contributes to an increasingly bulk-liquid-water-like network of H-bonds resulting in the decreasing difference between the hydration energy of LDH and the bulk liquid water energy. By $n = 4$, where the hydration energy of the formate−, acetate−, and propanoate−HTs converge, the H-bond requirements of all the -COO^- groups as well as that of the major fraction of the M−OH groups are essentially satisfied. With decreasing anion size from propanoate to formate, the fraction of the H-bonded M−OH groups increases from about 85 to 95% of its saturation value of 0.96/hydroxyl, which is independent of the anion. Thus, at this stage a well-developed, integrated H-bonding network is established between the interlayer species and the metal−hydroxide surface, as well as between the interlayer species themselves.

For water contents $n \geq 4$ the number of H-bonds accepted by the anions is essentially saturated, the added water molecules start hydrating the hydrophobic tails of the anions, continue to solvate the remaining M−OH groups, and replace H-bonds between the anions and the M−OH groups at a much slower

rate than at lower water contents. Simultaneously, the anions continue to rearrange in favor of vertical orientation with respect to the metal−hydroxide layers. Although solvation of the hydrophobic tails is energetically unfavorable, solvation of the M−OH groups is favorable. The contributions of these two processes are proportional to the size of the hydrophobic groups. The similarity of the hydration energy for the different monocarboxylate species, thus, suggests that the energetic effects of these two processes are mutually compensating. The net result of hydration over the range of $4 \leq n \leq 10$ is the gradual development of an improved, well-interconnected and less strained, H-bonding network resulting in rather slow variation in the hydration energy toward the saturation value.

There are significant differences between the behavior of monocarboxylate anions and tricarboxylate citrate in HT interlayers. The presence of the three carboxylate groups on a fairly rigid carbon backbone makes it more difficult for citrate to accept a sufficient number of H-bonds from the essentially rigid metal−hydroxide layers. Thus, there is a higher degree of incommensurability for the citrate with respect to the HT layers, which is reflected in its relatively low H-bond acceptance in the dry state. This structure also favors the acceptance of H-bonds from water. This preference of the -COO^- groups for H-bonds from H_2O rather than M−OH occurs despite the fact that the hydrogens of H_2O carry somewhat lower effective charges ($+0.41 \mid e \mid$) than those of M−OH ($+0.425 \mid e \mid$) in the model employed.[29] Thus, water molecules allow for more efficient solvation of -COO^- of the citrate and form more compact hydration shells leading to the slower basal expansion of citrate−HT with increasing water content.

4. Conclusions

The hydration energies of hydrotalcite containing the monocarboxylic anions formate, acetate, and propanoate computed from MD simulations over a wide range of water contents exhibit a slow approach to bulk liquid water value, with no well-defined minima at specific water contents. This behavior is in good qualitative agreement with previous molecular dynamics studies of citrate−HT.[21] It suggests that hydrotalcites intercalated with carboxylate anions, unlike most inorganic−HTs, do not have energetically well-defined structural states at specific water contents but, rather, absorb water in a continuous fashion in water-rich environments such as at high relative humidity or in aqueous suspensions. This conclusion is consistent with the recent experimental observation of the delamination of lactate− and citrate−HT.[16,17,20]

There are, however, significant quantitative differences in the behavior of hydrotalcites loaded with monocarboxylate anions and tricarboxylate citrate, and analysis of the interlayer structure and hydrogen-bonding provides an understanding of the origin of these differences. The swelling behavior of all these phases is due largely to the affinity of the -COO^- groups for H-bonds donated by water molecules, which can better solvate the -COO^- groups than the fixed M−OH sites of the hydroxide layers. Thus, the H-bond network is much better interconnected and less strained when water is present than in the dry phase. The superior swelling behavior (more negative hydration energy) of citrate−HT is due to a combination of factors including greater incommensurability of citrate with the hydroxide layers, the ability of citrate to form stronger and more compact hydration shells due to its higher charge, and the resulting slower basal expansion under hydration. The MD results here, thus, suggest that the swelling behavior and delamination of layered double hydroxides in water can be improved by starting with larger interlayer species with multiple carboxylic sites.

Acknowledgment. This research was supported by DOE Basic Energy Sciences Grant DEFGO2-00ER-15028. Computations were partially supported by the National Center for Supercomputing Applications (Grant EAR 990003N) and utilized Cerius2-4.9 software package from Accelrys, Inc.

References and Notes

(1) *Layered Double Hydroxides: Present and Future*; Rives, V., Ed.; Nova Science: New York, 2001; p 115.

(2) Braterman, P. S.; Xu, Z. P.; Yarberry, F. Chemistry of layered double hydroxides. In *Handbook of Layered Materials*; Auerbach, S. A., Carrado, K. A., Dutta, P. K., Eds.; Dekker: New York, 2004; pp 373−475.

(3) Newman, S. P.; Jones, W. *New J. Chem.* **1998**, 105.

(4) Evans, D. G.; Duan, X. *Chem. Commun. (Cambridge)* **2006**, 485.

(5) Kannan, S. *Catal. Surv. Asia* **2006**, *10*, 117.

(6) Leroux, F.; Taviot-Guého, C. *J. Mater. Chem.* **2005**, *15*, 3628.

(7) Del Hoyo, C. *Appl. Clay Sci.* **2007**, *36*, 103.

(8) Choy, J.-H.; Choi, S.-J.; Oh, J.-M.; Park, T. *Appl. Clay Sci.* **2007**, *36*, 122.

(9) Khan, A. I.; O'Hare, D. *J. Mater. Chem.* **2002**, *12*, 3191.

(10) Williams, G. R.; O'Hare, D. *J. Mater. Chem.* **2006**, *16*, 3065.

(11) Khan, A. I.; Lei, L.; Norquist, A. J.; O'Hare, D. *Chem. Commun. (Cambridge)* **2001**, 2342.

(12) Ambrogi, V.; Fardella, G.; Grandolini, G.; Perioli, L. *Int. J. Pharm.* **2001**, *220*, 23.

(13) Kwak, S.-Y.; Kriven, W. M.; Wallig, M. A.; Choy, J.-H. *Biomaterials* **2004**, *25*, 5995.

(14) Del Arco, M.; Cebadera, E.; Gutiérres, S.; Martín, C.; Montero, M. J.; Rives, V.; Rocha, J.; Sevilla, M. A. *J. Pharm. Sci.* **2004**, *93*, 1649.

(15) Mohanambe, L.; Vasudevan, S. *J. Phys. Chem. B* **2005**, *109*, 15651.

(16) Hibino, T.; Kobayashi, W. *J. Mater. Chem.* **2005**, *15*, 653.

(17) Jaubertie, C.; Holgado, M. J.; San Roman M. S.; Rives, V. *Chem. Mater.* **2006**, *18*, 3114.

(18) Adachi-Pagano, M.; Forano, C.; Besse, J.-P. *Chem. Commun. (Cambridge)* **2000**, *91*.

(19) Leroux, F.; Adachi-Pagano, M.; Intissar, M.; Chauvière, S.; Forano, C.; Besse, J.-P. *J. Mater. Chem.* **2001**, *11*, 105.

(20) Li, Q.; Kirkpatrick, R. J. *Am. Mineral.* **2007**, *92*, 397.

(21) Kumar, P. P.; Kalinichev, A. G.; Kirkpatrick, R. J. *J. Phys. Chem. B* **2006**, *110*, 3841.

(22) Reinholdt, M. X.; Kirkpatrick, R. J. *Chem. Mater.* **2006**, *18*, 2567.

(23) Kirkpatrick, R. J.; Reinholdt, M. X.; Kalinichev, A. G. *Geochim. Cosmochim. Acta* **2005**, *69*, A44.

(24) Hou, X.; Bish, D. L.; Wang, S.-L.; Johnston, C. T.; Kirkpatrick, R. J. *Am. Mineral.* **2003**, *88*, 167.

(25) Bellotto, M.; Rebours, B.; Clause, O.; Lynch, J.; Bazin, D.; Elkaïm, E. *J. Phys. Chem.* **1996**, *100*, 8527. Bellotto, M.; Rebours, B.; Clause, O.; Lynch, J.; Bazin, D.; Elkaïm, E. *J. Phys. Chem.* **1996**, *100*, 8535.

(26) Vucelic, M.; Jones, W.; Moggridge, G. D. *Clays Clay Miner.* **1997**, *45*, 803.

(27) Génin, J.-M. R; Abdelmoula, M.; Aïssa, R.; Ruby, C. *Hyperfine Interact.* **2005**, *166*, 391.

(28) Lide, D. R., Ed. *CRC Handbook of Chemistry and Physics*, 87th ed.; CRC Press: Boca Raton, FL, 2006; p 8−42.

(29) Cygan, R. T.; Liang, J.-J.; Kalinichev, A. G. *J. Phys. Chem. B* **2004**, *108*, 1255.

(30) Berendsen, H. J. C.; Postma, J. P. M.; van Gunsteren, W. F.; Hermans, J. Interaction models for water in relation to protein hydration. In *Intermolecular Forces*; Pullman, B., Ed.; Riedel: Dordrecht, The Netherlands, 1981; p 331.

(31) Kitson, D. H.; Hagler, A. T. *Biochemistry* **1988**, *27*, 5246.

(32) Perry, T. D., IV; Cygan, R. T.; Mitchell, R. *Geochim. Cosmochim. Acta* **2006**, *70*, 3508.

(33) Xu. X.; Kalinichev, A. G.; Kirkpatrick, R. J. *Geochim. Cosmochim. Acta* **2006**, *70*, 4319.

(34) Smith, D. E. *Langmuir* **1998**, *14*, 5959.

(35) Wang, J.; Kalinichev, A. G.; Kirkpatrick, R. J.; Hou, X. *Chem. Mater.* **2001**, *13*, 145.

(36) Heinz, H.; Koerner, H.; Vaia, R. A.; Anderson, K. L.; Farmer, B. L. *Chem. Mater.* **2005**, *17*, 5658.

(37) Luzar, A.; Chandler, D. *Phys. Rev. Lett.* **1996**, *76*, 928.

(38) Kalinichev, A. G.; Kirkpatrick, R. J. *Chem. Mater.* **2002**, *14*, 3539.

(39) Wang, J.; Kalinichev, A. G.; Kirkpatrick, R. J. *Geochim. Cosmochim. Acta* **2006**, *70*, 562.

(40) Boek, E. S.; Coveney, P. V.; Skipper, N. T. *J. Am. Chem. Soc.* **1995**, *117*, 12608.